

RESEARCH ARTICLE

Electroretinographic evidence suggesting that the type 2 diabetic retinopathy of the sand rat *Psammomys obesus* is comparable to that of humans

Ahmed Dellaa^{1,2}, Maha Benlarbi¹, Imane Hammoum¹, Nouha Gammoudi³, Mohamed Dogui³, Riadh Messaoud⁴, Rached Azaiz⁵, Ridha Charfeddine⁵, Moncef Khairallah⁴, Pierre Lachapelle⁶, Rafika Ben Chaouacha-Chekir^{1*}

1 Laboratory of Physiopathology, Food and Biomolecules of the Higher Institute of Biotechnology Sidi Thabet, Manouba University, BiotechPole Sidi Thabet, Ariana, Tunisia, **2** Faculty of Sciences of Bizerte, Carthage University, Bizerte, Tunisia, **3** Department of functional explorations of the nervous system, University Hospital of Sahloul, Sousse, Tunisia, **4** Department of Ophthalmology, University Hospital of Fattouma Bourguiba, Monastir, Tunisia, **5** UNIMED Pharmaceutical Industry, industrial area Kalaa Kebira, Sousse, Tunisia, **6** Department of Ophthalmology, Research Institute of the McGill University Health Centre, Montreal, Quebec, Canada

* raf_chekir@yahoo.fr



OPEN ACCESS

Citation: Dellaa A, Benlarbi M, Hammoum I, Gammoudi N, Dogui M, Messaoud R, et al. (2018) Electroretinographic evidence suggesting that the type 2 diabetic retinopathy of the sand rat *Psammomys obesus* is comparable to that of humans. PLoS ONE 13(2): e0192400. <https://doi.org/10.1371/journal.pone.0192400>

Editor: Radouil Tzekov, Roskamp Institute, UNITED STATES

Received: April 28, 2017

Accepted: January 23, 2018

Published: February 8, 2018

Copyright: © 2018 Dellaa et al. This is an open access article distributed under the terms of the [Creative Commons Attribution License](https://creativecommons.org/licenses/by/4.0/), which permits unrestricted use, distribution, and reproduction in any medium, provided the original author and source are credited.

Data Availability Statement: All relevant data are within the paper and its Supporting Information files.

Funding: This work was done within the MOBIDOC program launched under the Support Project to the Research and Innovation System (PASRI) funded by the European Union (EU) and managed by the National Agency for the Promotion of Scientific Research (ANPR) in partnership with UNIMED Laboratories, <http://www.pasri.tn/>. The funders had

Abstract

Purpose

Type 2 diabetic retinopathy is the main cause of acquired blindness in adults. The aim of this work was to examine the retinal function of the sand rat *Psammomys obesus* as an animal model of diet-induced type 2 diabetes when subjected to a hypercaloric regimen.

Materials and methods

Hyperglycemia was induced in *Psammomys obesus* by high caloric diet (4 kcal/g). The visual function of control (n = 7) and diabetic (n = 7) adult rodents were followed up during 28 consecutive weeks with full-field electroretinogram (ERG) recordings evoked to flashes of white light according to the standard protocol of the International Society for Clinical Electrophysiology of Vision protocol (ISCEV).

Results

Twenty-eight weeks following the induction of diabetes, results revealed significantly reduced and delayed photopic and scotopic ERG responses in diabetic rats compared to control rats. More specifically, we noted a significant decrease in the amplitude of the dark-adapted 0.01 ERG (62%), a- and b-wave amplitudes of the dark-adapted 3.0 ERG (33.6%, 55.1%) and the four major oscillatory potentials components (OP1-OP4) (39.0%, 75.2%, 54.8% and 53.7% respectively). In photopic conditions, diabetic rats showed a significant decrease in a- and b-wave (30.4%, 43.4%), photopic negative response (55.3%), 30 Hz flicker (63.7%), OP1-OP4 (51.6%, 61.8%, 68.3% and 47.5% respectively) and S-cone

no role in study design, data collection and analysis, decision to publish, or preparation of the manuscript. UNIMED Laboratories provided support in the form of salaries for author AD, but did not have any additional role in the study design, data collection and analysis, decision to publish, or preparation of the manuscript. The specific roles of these authors are articulated in the 'author contributions' section.

Competing interests: Support from UNIMED Laboratories does not alter our adherence to PLOS ONE policies on sharing data and materials.

(34.7%). Significantly delayed implicit times were observed for all ERG components in the diabetic animals. Results obtained are comparable to those characterizing the retinal function of patients affected with advanced stage of diabetic retinopathy.

Conclusion

Psammomys obesus is a useful translational model to study the pathophysiology of diabetic retinopathy in order to explore new therapeutic avenues in human patients.

Introduction

Diabetic retinopathy (DR), which can lead to blindness in severe cases, is reported to affect more than 90% of diabetic patients [1]. The pathophysiology of diabetic retinopathy is believed to result from the sustained exposure to hyperglycemia which leads to retinal biochemical abnormalities [2]. In addition, although DR has long been recognized as a vascular disease [3–5], the neuronal cells of the retina are also affected [6–10]. Supportive of the latter, previous studies reported that some visual anomalies such as color vision deficits [11, 12] or decreased contrast sensitivity [13] precede the vascular signs of DR, suggesting that the vascular abnormalities may not be the first sign characterizing the onset of DR [14, 15]. Similarly, it was previously shown that flash and multifocal electroretinograms can detect retinal neurosensory changes long before an observable retinopathy occurs [16–18]. For instance, it was shown that the onset of the proliferative phase of diabetic retinopathy was better predicted with the selective amplitude reduction of the oscillatory potentials of the ERG than with the vascular lesions seen in fundus photographs [19, 20]. Clinical studies have also shown that retinal ganglion cells (RGC) and neuronal activity progressively decreases with advancing DR as indicated by the photopic negative response (PhNR) that follows the photopic ERG b-wave [14]. Chemically-induced diabetes was also shown to yield early functional changes in the retina, such as in streptozotocin (STZ)-treated rodents [21–24] and alloxan-treated rabbits [25, 26].

We have previously shown that sand rats *Psammomys obesus* (*P.obesus*) fed with a high caloric diet will spontaneously develop type 2 diabetes, with accompanying retinopathy, thus making them a valid translational model of this retinal disorder [27]. Animals subjected to this regimen typically develop hyperglycemia and severe DR-like ocular complications such as vascular alterations, elevated vitreous ratios of pro- and anti-angiogenic growth factors, blood-retinal barriers structure breakdown and neural and glial changes similar to the ones occurring in humans [27, 28]. The purpose of this study was to investigate if the diabetes-induced retinal functional changes observed in *P.obesus* also compare with what is reported in diabetic human subjects.

Materials and methods

Animals

P.obesus was captured in a semi-desertic area of southern Tunisia in Gafsa (National Park of Bou-Hedma), in strict accordance with the national regulations on the treatment of wildlife. All *P.obesus* were housed in standard animal housing rooms on 12/12-hour light/dark cycle with food and water *ad libitum*. The room temperature and relative humidity was set simultaneously at 24°C ± 1°C and 70% ± 5%. Only male rats were used in this study. Data for this study came from 14 adult males separated into two groups. The control group (n = 7) received

a natural hypocaloric (0.4 kcal/g wet weight) vegetable diet, i.e., halophilic plants (Chenopodiaceae), rich in water and mineral salts. The diabetic group ($n = 7$) received a standard laboratory rat enriched chow feed (4 kcal/g) and mineral water *ad libitum*. The animals were followed up for a maximum of 7 months with measurements of body weight and plasmatic glucose. All procedures adhered to the ARVO Statement for the Use of Animals in Ophthalmic and Vision Research and approved by the local Bio-Medical Ethic Committee of Pasteur Institute of Tunis (protocol # 2016/11/E/ISBST/V1). *P.obesus* was captured according to the rules authorization of Tunisian Agriculture Ministry (ref. 2016/1693).

Electroretinography

Measurements were made as described in our previous study [29]. Briefly, the visual monitor system (Mon Color, Metrovision) was used for stimulus generation and data acquisition. *P. obesus* were dark-adapted overnight, and the experimental procedure was done under a dim-red light (<1 Lux). Animals were anesthetized with an intraperitoneal injection of ketamine (120 mg/kg). The pupils were dilated using tropicamide (25mg/5ml; UNIMED, Tunisia) and the cornea was anesthetized with a drop of 0.5% Alcaine. For all animals, the ERG was recorded with a DTL fiber electrode (X-static silver coated conductive nylon yarn, Sauquoit Industries, Scranton, PA, USA) maintained on the cornea with one drop of tear gel (Lacryvisc, Carbomer 974 P, Alcon), to prevent corneal dryness. The reference and ground stainless steel needle electrodes were inserted subcutaneously on the forehead and tail, respectively. The five standard ERG responses advocated by the International Society for Clinical Electrophysiology of Vision (ISCEV) were used to compare the retinal function of the control and diabetic *P.obesus* as well as human subjects [30].

The scotopic ERG responses (Amplification: $\times 12500$; 1–1200 Hz bandwidth) were evoked to flashes of white light of 0.01cd.s/m^2 (rod responses) and 3cd.s/m^2 (mix rod-cone response and oscillatory potentials: OPs). Oscillatory potentials were obtained by Fourier transform using an 80–200 Hz bandwidth which is a software filter built in the instrument. Following the scotopic recordings and after 10 minutes of light-adaptation (30cd.m^{-2} background light), photopic (cone-mediated) ERGs were evoked using flashes of white light of 3cd.s/m^2 in intensity. Each set of ERG responses was an average of 20 responses evoked at an inter-stimulus interval of 1 second [29]. A 30-Hz flicker response was also obtained using the same flash intensity and background. The S-cone response was obtained to a violet flash (414 nm) stimulus with intensity of 0.0045cd s/m^2 delivered against a red-orange (595 nm) background 150cd.m^{-2} to suppress the contribution of rods and M cones.

Data analysis

ERG analysis was performed according to the standard practice [30] as previously reported [29]. The following ERG parameters were measured: rod-response amplitude (from the baseline to positive peak), a-wave amplitude (baseline to the first negative deflection), b-wave amplitude (a-wave peak to positive b-wave peak), i-wave amplitude (from the trough of the b-wave to the peak of the i-wave), PhNR amplitude (baseline to negative trough following b-wave), 30 Hz flicker amplitude (from the trough to the peak), OPs amplitude (the sum amplitude of wavelets 1–4 measured from the trough to the peak of each response component), S-cone amplitude (the b-wave amplitude of the S-cone response was quantified) and the b/a-wave amplitude ratio. All peak times were measured from the flash onset to the peak of each component.

Data was expressed as means \pm standard error of mean (SEM). Comparison findings between groups were done using the Mann-Whitney test. Differences were considered

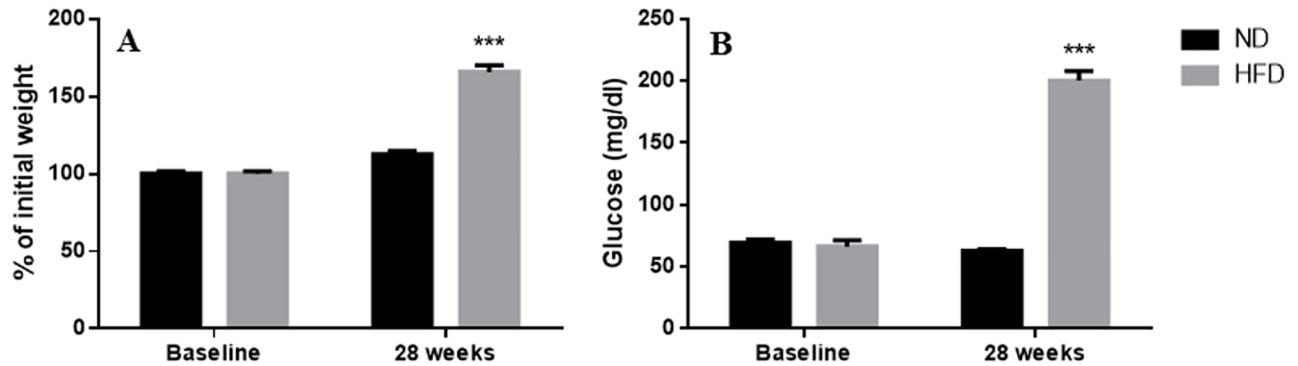


Fig 1. Body weight in % of initial weight (A) and blood glucose (B) parameters before and after normal diet (ND; N = 7 *P.ob*) and high fat diet (HFD; N = 7 *P.ob*) feeding during 28 weeks in *Psammomys obesus*. Values are given as means \pm SEM. *** $p \leq 0.001$. Control (black trace); Diabetic (grey trace).

<https://doi.org/10.1371/journal.pone.0192400.g001>

statistically significant when the p -values were less than 0.05. All statistical analyses were performed with GraphPad Prism (GraphPad Software Inc., San Diego, USA).

Results

Diabetes affects biological parameters

At Fig 1 the average body weight in % (A) and blood glucose parameters levels (B) obtained measured 28 weeks following the induction of diabetes are presented. At the baseline, the body weight and blood glucose levels were similar between the two groups. Twenty-eight weeks of high-fat diet increased body weight by 65.9% compared to the baseline and by 12.6% compared with control-fed on with the natural diet. Similarly, the blood glucose level was significantly increased (200.3 ± 7.7 vs 62.7 ± 1.6 mg/dl; $p = 0.0006$) in the high-fat diet group compared to the natural diet group.

The effect of diabetes progression on the ERG

As illustrated in Fig 2 (and summarized in Table 1), our results show that following 28 weeks of diabetes all the ERG components of the photopic and scotopic responses (including the

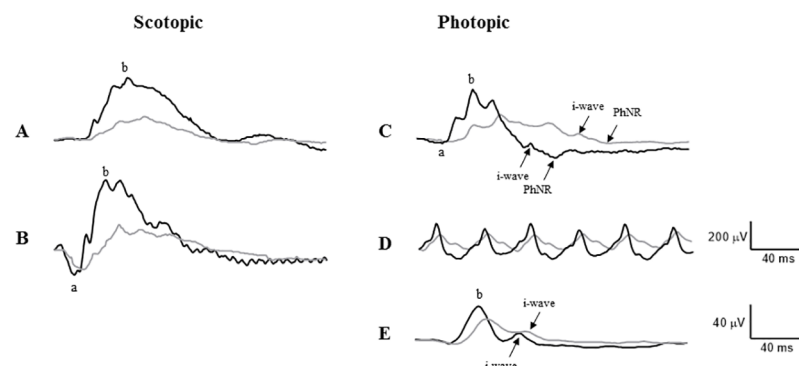


Fig 2. Retina function (electretinograms) of *Psammomys obesus*, control and diabetic, at 28 weeks following the onset of diabetes. Representative traces indicating: (A) Rod responses using 0.01 cd.s/m^2 flash. (B) mixed response using 3 cd.s/m^2 flash. (C) Photopic responses using 3 cd.s/m^2 flash. (D) Photopic 30 Hz flicker response. (E) Photopic S-cone response using 0.0045 cd.s/m^2 blue flash on an orange background. Individual waveform components are indicated in parentheses. Black traces—responses from control animals, Grey traces—from diabetic. For more details, see main text.

<https://doi.org/10.1371/journal.pone.0192400.g002>

Table 1. ERG components for control and diabetic *Psammomys obesus*.

ERG Parameters	Control (n = 7)	Diabetic (n = 7)	p-values
Rod response			
Amplitude ^α	398.8 ± 22.2	146.1 ± 4.1	*** 0.0006
Implicit time ^β	53.1 ± 1.3	61.4 ± 2.4	** 0.01
Scotopic b-wave			
Amplitude	647.1 ± 25.4	290.7 ± 11.5	*** 0.0006
Implicit time	35.0 ± 1.9	49.6 ± 2.7	*** 0.007
Scotopic a-wave			
Amplitude	163.1 ± 6.5	108.5 ± 9.8	*** 0.0006
Implicit time	14.0 ± 0.5	21.0 ± 0.4	*** 0.0006
Scotopic b-/a- wave amplitude ratio	4.0 ± 0.2	2.8 ± 0.2	*** 0.002
Dark-adapted OP			
OP1 amplitude	29.7 ± 3.4	16.9 ± 0.6	** 0.01
OP2 amplitude	136.6 ± 7.0	32.4 ± 9.4	*** 0.0006
OP3 amplitude	117.3 ± 17.2	43.7 ± 6.8	*** 0.002
OP4 amplitude	59.1 ± 9.0	25.8 ± 4.0	*** 0.002
Sum OP amplitude	342.8 ± 30.5	117.0 ± 18.2	*** 0.0006
OP1 implicit time	14.2 ± 0.1	16.3 ± 0.6	** 0.01
OP2 implicit time	22.9 ± 0.5	28.1 ± 0.7	*** 0.006
OP3 implicit time	32.3 ± 0.8	38.3 ± 1.3	*** 0.002
OP4 implicit time	43.1 ± 0.8	49.4 ± 4.6	** 0.01
Photopic a-wave			
Amplitude	28.1 ± 1.1	19.4 ± 0.6	*** 0.001
Implicit time	15.9 ± 0.3	20.4 ± 0.7	**** 0.0001
Photopic b-wave			
Amplitude	308.3 ± 22.4	169.7 ± 24.6	*** 0.007
Implicit time	39.1 ± 0.7	60.2 ± 6.3	*** 0.0006
Photopic b-/a- wave amplitude ratio	11.1 ± 1.1	8.7 ± 1.1	0.1
i-wave			
Amplitude	27.1 ± 3.1	12.4 ± 0.7	* 0.04
Implicit time	78.5 ± 1.5	107.8 ± 8.8	*** 0.008
PhNR			
Amplitude	88.4 ± 7.4	37.8 ± 4.4	*** 0.002
Implicit time	97.5 ± 1.8	133.9 ± 7.7	*** 0.004
Photopic adapted OP			
OP1 amplitude	24.1 ± 1.8	11.2 ± 0.6	*** 0.001
OP2 amplitude	48.1 ± 6.7	17.4 ± 1.0	*** 0.0006
OP3 amplitude	54.9 ± 4.3	16.6 ± 2.5	*** 0.0006
OP4 amplitude	43.8 ± 10.1	18.1 ± 3.6	** 0.01
Sum OP amplitude	170.9 ± 17.7	63.3 ± 6.1	*** 0.0006
OP1 implicit time	16.4 ± 0.8	25.2 ± 1.0	*** 0.0006
OP2 implicit time	27.4 ± 0.8	35.3 ± 0.5	*** 0.001
OP3 implicit time	37.4 ± 0.7	45.4 ± 2.1	*** 0.001
OP4 implicit time	48.3 ± 1.2	56.6 ± 3.8	** 0.06
30-Hz flicker			
Amplitude	293.6 ± 16.4	105.7 ± 7.3	*** 0.0006
Implicit time	34.1 ± 0.2	36.5 ± 0.4	** 0.01
Photopic S-cone			

(Continued)

Table 1. (Continued)

ERG Parameters	Control (n = 7)	Diabetic (n = 7)	p-values
Amplitude	41.8 ± 5.2	27.1 ± 3.1	*** 0.001
Implicit time	43.4 ± 0.7	50.5 ± 2.3	** 0.01

^aAmplitude is in microvolts (μV)

^bImplicit time is in milliseconds (ms)

Data are expressed as the mean ± SEM.

* $p \leq 0.05$

** $p \leq 0.01$

*** $p \leq 0.001$

**** $p \leq 0.0001$

<https://doi.org/10.1371/journal.pone.0192400.t001>

scotopic but not the photopic b/a wave ratios) were significantly attenuated (S7–S12 Figs) and delayed compared to control (S1–S6 Figs).

Fig 3 displays the percentage of diabetes-induced amplitude decrease in different ERG components. Compared to the control group, the amplitude of the rod-response and the mixed a-wave and b-wave (rod-cone) decreased significantly by 62.6% ($p = 0.0006$), 33.6% ($p = 0.0006$) and 55.1% ($p = 0.0006$), respectively (Table 2). Likewise, in photopic conditions the amplitude of a-, b-, i-wave, PhNR, flicker and S-cone were also significantly decreased between 30.4% and 68% (Table 2). There were no significant differences in the amount of diabetes-induced amplitude reductions when photopic and scotopic ERG components were compared (Table 3).

Results obtained with the OPs of control and diabetic *P.obesus* are presented at Fig 4. The summed amplitude of the scotopic OPs in diabetic *P.obesus* was approximately 62% smaller than control. When considered individually, the amplitudes of all OPs (OP1-OP4) were significantly ($p \leq 0.05$) reduced by 39.0%, 75.1%, 54.8% and 53.7% respectively. Similarly, the

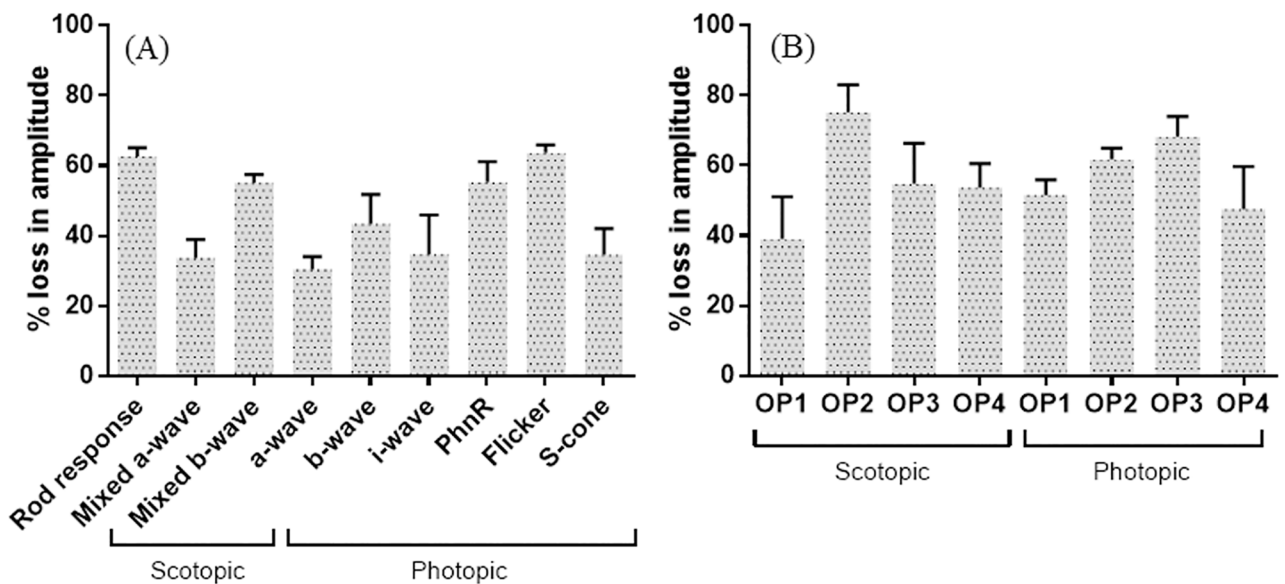


Fig 3. Percentage loss of amplitude in various ERG waveforms in diabetic *P.obesus* after 28 weeks. Left panel (A) indicates changes in main wave form parameters; right panel (B) indicates changes in individual oscillatory wavelets. Each bar graph indicates average ± SEM.

<https://doi.org/10.1371/journal.pone.0192400.g003>

Table 2. The amplitudes percentage decrease in various ERG waveforms in diabetic *P.obesus* compared to control group.

ERG waveforms	Percentage loss in amplitude (%)
Scotopic condition	
Rod response	62.6 ± 2.5
Mixed a-wave	33.6 ± 5.3
Mixed b-wave	55.1 ± 2.4
OP1	39.0 ± 12.1
OP2	75.2 ± 7.9
OP3	54.8 ± 11.6
OP4	53.7 ± 6.8
Sum OP	63.8 ± 7.1
Photopic condition	
a-wave	30.4 ± 3.6
b-wave	43.4 ± 8.4
i-wave	34.7 ± 11.2
PhNR	55.3 ± 5.9
Flicker	63.7 ± 2.2
S-cone	34.7 ± 7.4
OP1	51.6 ± 4.3
OP2	61.8 ± 3.1
OP3	68.3 ± 5.7
OP4	47.5 ± 12.2
Sum OP	60.9 ± 4.9

<https://doi.org/10.1371/journal.pone.0192400.t002>

amplitudes of all photopic OPs (OP1- OP4) were significantly ($p \leq 0.05$) reduced by 51.6%, 61.8%, 68.3% and 47.5% respectively, as well as delayed implicit time of each oscillatory potential peak were noted (Fig 2; Table 1).

As shown in Table 3, there were no significant differences in the DR-induced amplitude reduction measured when the photopic and scotopic a-waves, b-waves and OPs were compared to each other. Similarly, when considering the scotopic response, both a-and b-waves were similarly attenuated and the same was also observed with the photopic response.

Table 3. Comparison between percentage change in amplitude of different ERG components.

Comparison	p-value	Comparison	p-value
Photopic vs scotopic responses		Other responses b-wave vs a-wave	
a-wave	0.52	Scotopic a-wave vs b-wave	0.07
b-wave	0.96	Photopic a-wave vs b-wave	0.18
OP1	0.66	Slow waves vs fast waves	
OP2	0.14	Scotopic a-wave vs sum OP	*0.01
OP3	0.31	Scotopic b-wave vs sum OP	0.05
OP4	0.66	Photopic a-wave vs sum OP	**0.001
		Photopic b-wave vs sum OP	0.16

* $p \leq 0.05$

** $p \leq 0.01$

N = 7 diabetic *P.obesus*.

<https://doi.org/10.1371/journal.pone.0192400.t003>

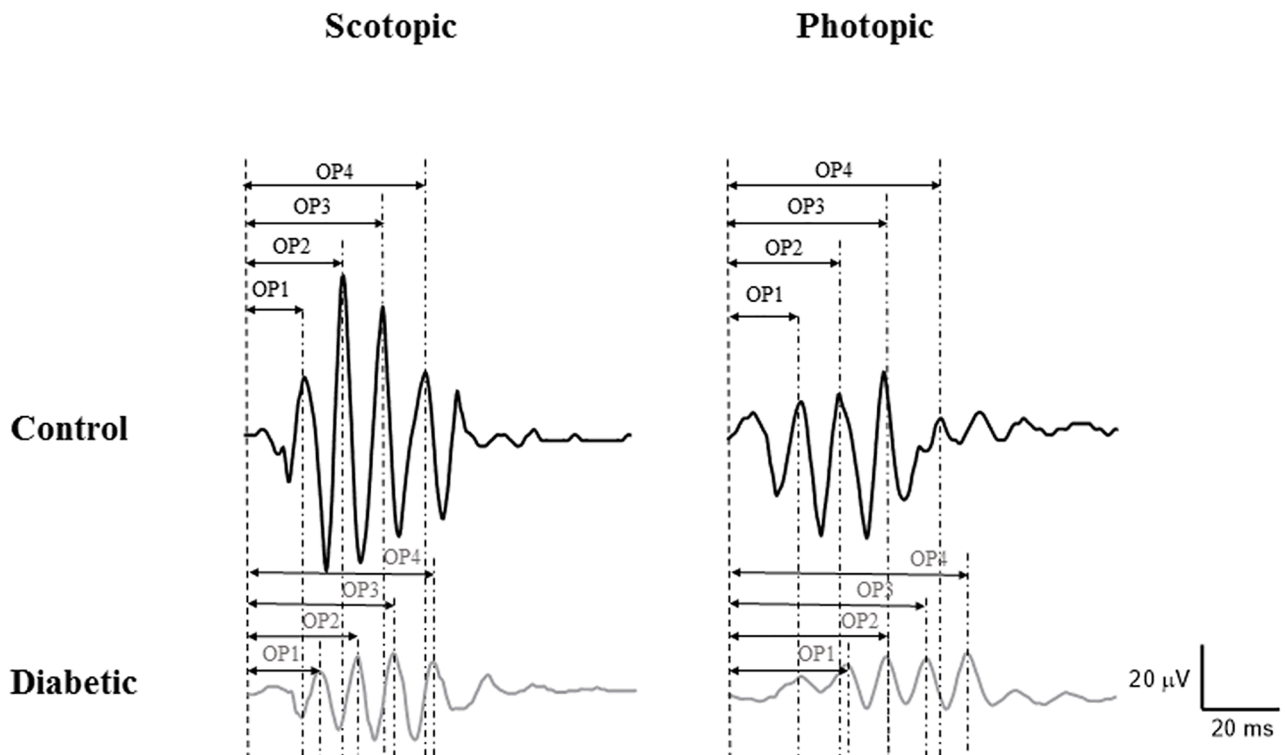


Fig 4. Individual representative of oscillatory potentials recorded from control and diabetic *P.obesus*. Ops were recorded in response to 3 cd.s/m² flash under scotopic and photopic conditions. The OPs have been enumerated on each trace. Control (black trace); Diabetic (grey trace). Horizontal calibration, 20 ms; vertical calibration, 20 μ V.

<https://doi.org/10.1371/journal.pone.0192400.g004>

However, of interest, while the DR-induced attenuation of the photopic and scotopic a-waves appeared to be significantly different from that of the corresponding OPs, photopic and scotopic b-waves and corresponding OPs were similarly attenuated. The latter would suggest that DR differentially affects the outer (a-wave) and inner (OPs more than b-wave) retina, regardless of the state of retinal adaptation.

Discussion

P.obesus maintained on a high-fat diet for 28 consecutive weeks developed hyperglycemia with body weight increase as reported in a previous study of ours [31]. This high-fat diet induced a metabolic stress syndrome in *P.obesus* which led to an alteration to the retinal structure [31]. The present study demonstrated that this alteration to the retinal structure is paralleled by an equally profound deterioration in retinal function (decrease in amplitude scotopic and photopic a- and b-waves, OP1-OP4 components, PhNR, Flicker and S-cone).

Electrophysiological evaluation after the morphological assessment in diabetic *P.obesus* [27] was needed to clarify the functional changes in the photoreceptor cells of diabetic retina. Several studies used the *P.obesus* as an experimental model to study metabolic dysfunction leading to diabetes and its complications such as nephropathy, cardiomyopathy and retinopathy [27, 32, 33]. These metabolic and endocrine disorders are comparable to those observed in humans with type 2 diabetes. Our recent work [27] on the molecular and cellular alterations showed that the DR of *P.obesus* is similar to those reported in diabetic patients. Similarly, the electroretinogram of *P.obesus* also shares several features with that of human subjects [29], making it a remarkable model to investigate the retinal complications of diet-induced type 2 DR as it

meets the criteria listed by the AMDCC [Animal models of diabetic complications consortium (www.amdcc.org)]. Of interest, in the present study, all *P.obesus* which developed DR after 28 weeks of high-fat treatment also developed a retinal dysfunction as measured with the ERG.

Impairment of scotopic and photopic ERG parameters

Our results demonstrated that the amplitude of a- and b- waves ERG of diabetic rodents at 28 weeks were significantly reduced, and the implicit times were considerably delayed compared to control *P.obesus*. These functional changes suggest that photoreceptor function, as well as synaptic transmission from the photoreceptors to bipolar cells, were affected *in vivo* by the high-fat induced hyperglycemia [27, 34]. The morphological findings after 7 months of diabetes in *P.obesus* showed a decreased expression of both PKC α and ζ isoforms that are Ca²⁺ independent and co-localized in rod bipolar cells [27]. This decreased expression may be related to photoreceptor alterations in diabetic *P.obesus* retina. Another alteration detected in diabetic retina in our previous study affecting the synaptic terminals by an increase in synaptic proteins such as synaptophysin [27]. The upregulation of GFAP in Müller cells has been demonstrated in the retinas of *P.obesus* viewed as an indicator of retinal cell stress [27]. These changes, in combination with high blood glucose may unpair the function of these cells. Likewise, a high concentration of glucose can promote photoreceptor degeneration as demonstrated *in vitro* by Baccouche et al. [35]. ERG abnormalities found in the diurnal *P.obesus* were present for both scotopic (rod-mediated) and photopic (cone-mediated) conditions, indicating that both retinal systems are affected in our animal model of diabetic retinopathy. Based on ERG abnormalities and histologic findings in advanced human DR, a significant decrease in amplitudes of scotopic a- and b- waves from pre-proliferative DR [36] indicates impairment of the outer segments of the photoreceptors [37]. The dark-adapted ERG [38] is reported to be more impaired compared to the light-adapted ERG [39–41]. Thus, in rod dominated retinas, e.g. some rodents (97% rods in rats and mice) and peripheral human retina (96% rods), scotopic conditions that selectively measure rod responses allow easy detection of functional deficits [42]. Chung et al. [36] reported less temporal variability compared to amplitude variability of ERG and a significant prolonged b-wave implicit time at all stages of retinopathy and in the eyes of diabetic patients without retinopathy. Similar results have been observed in streptozotocin-induced diabetic rats [43–46] and in our model diabetics of *P.obesus* at 28 weeks after diabetes induction. A calculation of b-/a-wave amplitude ratios in the present study revealed a decline in scotopic condition, suggesting that bipolar cells are more affected than photoreceptors. However, in photopic condition the unchanged ratio showed that the decrease of b-wave amplitude was correlated to the photoreceptor response.

Impairment of individual OP wavelets

Our results also provide evidence of retinal impairments beyond the level of the photoreceptors in rodents with diabetes, given that OPs were shown to signal inner retinal activity, particularly the amacrine cells [47, 48]. Alteration of OPs in diabetic *P.obesus* may be explained by the loss of amacrine cell numbers at different cell retinal layers including retinal ganglion cells [27]. These changes were accompanied by an increase of immunohistochemical staining of tyrosine hydroxylase in amacrine cells of diabetes animals in comparison with control animals. As previously shown with clinical and experimental data [14, 49–51], the OPs are significantly altered in advanced stages of diabetes. The reduction in amplitude and delay in implicit time for each OP of the diabetic *P.obesus* ERG were comparable to what is reported in human patients at the proliferative stage in diabetic retinopathy [52–54]. This study confirms the

previously reported link between attenuated and delayed OPs and severity of diabetic retinopathy in patients [19, 20, 55–57], a feature also observed in *P.obesus*.

Currently available diabetic rodent models can be used to study the initial (acute) or latent phase of diabetic retinopathy and several studies have reported a concurrent change in OPs [21, 58, 59]. For example, male Sprague-Dawley STZ rats showed an amplitude reduction of OP1 and OP2 after 6–20 weeks of diabetes induction [60]. However, contrasting with the above, spontaneous Torii rats showed a non-specific attenuation of all ERG components (i.e. a- and b-waves and the OPs) [15]. Our results thus show that our diet-induced diabetic type 2 *P.obesus* model mimics several of the DR features observed in human diabetes and should therefore be considered as a valid alternative to test therapeutic pharmacological molecules on type 2 DR functions.

i-wave in diabetic retinopathy

The i-wave of the human full-field photopic ERG response is a relatively small positive deflection following the b-wave and is thought to originate in an off-circuitry in the inner retina [61]. Although Rosolen et al. [62] were able to record an i-wave in several species (dog, cat, rabbit, minipig, monkey) they were not able to detect it in mice and rats. However, the i-wave was clearly detectable in the Mongolian gerbil (a mostly diurnal rodent) by Yang et al. [63]. As the Mongolian gerbil retina has a higher proportion of cone photoreceptors (~13% [64]) vs. rats (0.85–1.5% [65], [66]), it is likely that the i-wave is generated by a more sophisticated cone circuitry compared to the one present in the standard laboratory rats. In support of this view, our results clearly demonstrate presence of an i-wave in the sand rat, which is also a mostly diurnal rodent and has a larger proportion of cone photoreceptors (41% [31]). This post b-wave component, which is said to originate from the activity of the retinal ganglion cells, probably the off pathway [67] became affected in diabetic *P.obesus* after 7 months of diabetic induction.

Changes in PhNR

Degeneration of the retinal ganglion cells (RGC) and deterioration of the inner nuclear layer in the retinas of diabetic *P.obesus* were previously reported by our laboratory showing a reduction by 44% of RGCs in diabetic *P.obesus* retina after 7 months of diabetes progression [27]. In the present study, we show a ~57% decrease in amplitude of the PhNR which is consistent with the hypothesis that reduced ganglion cells function may also be an important component of the pathogenesis of diabetic retinopathy, given that this negative, post b-wave component of the ERG is claimed to signal electrical events evoked in part by the RGC [68, 69]. In human patients, PhNR of reduced amplitude and increased timing were found to strongly correlate with progression of DR [14, 70, 71]. In the present study, we found that the PhNR was the ERG wave among the most severely affected component, suggesting that it could represent a more sensitive detector of DR onset.

30 HZ flicker alteration

Our results also showed that the photopic flicker ERG of our diabetic *P.obesus* was reduced in amplitude and delayed in timing, similar to what was previously reported in human diabetes [56, 72, 73]. Similar timing delays have been reported for other vascular retinopathy such as central and branch retinal vein occlusions [1]. The timing delays in the flash ERG and flicker can be explained by reduction in retinal sensitivity. In human Satoh et al. [74] described that the photopic ERG response of diabetic patients showed a clear alteration of the implicit time and a correlation of the amplitude with the severity of the disease. Based on the data presented

in Table 2, a significant decrease has been reported in 30 Hz flicker. The reduction of flicker response seems to be the second more affected photopic component after OP 3. Based on data in Table 1, it also looks that the decrease in amplitude was more significant than delay in timing. Thus, it appears that photopic 30 Hz flicker amplitude flicker is a sensitive measure for the diet-induced DR progression in the *P.obesus*. Recognition of these defects will enhance our understanding of the pathophysiology of diabetic retinopathy.

S-cone sensitivity loss

Finally, as previously shown in diabetic human subjects [75, 76], the S-cone ERGs of diabetic *P.obesus* was significantly reduced in amplitude and delayed in timing. The cone short-wavelength opsin staining was detectably reduced in *P.obesus* diabetic retinas and this was confirmed by Western blot analysis in our previous study [27].

In summary, the totality of our findings regarding ERG presented in this report further confirms the similarity between the characteristics of retina changes in diabetic *P.obesus* and the corresponding changes in human DR and support the notion that it represents a valid translational model to study the retinal pathophysiological processes involved in the onset and progression of type 2 diabetic retinopathy.”

Clearly, more studies are needed to better correlate structural and functional changes in the diabetic retina of *P.obesus*. Such studies should include fundus photography, optical coherence tomography and fluorescein angiography in order to clarify to what extent the ERG findings correlate (precede or follow) with morphological changes in the retina.

Conclusion

The present study clearly demonstrated for the first time that long-lasting and significant alterations in visual function detected by full-field ERG take place after 28 weeks of diet-induced type 2 diabetes in the retina of the sand rat. Thus, the diabetic sand rat appears to be an animal model that mimics several important features of the human form of diabetic retinopathy.

Our results confirm the validity of the *P.obesus* as a useful translational model to study diet-induced type 2 diabetic retinopathy (induced, like in humans, with the increase intake of high caloric food). We strongly believe that adding this new model to the researchers' armamentarium will not only be instrumental in increasing our understanding of the pathophysiology of human diabetic retinopathy but also help in the development of new therapeutic strategies.

Supporting information

S1 Fig. Individual presentation of retina function (electroretinograms) of *Psammomys obesus*, control 1, at 28 weeks following the onset of diabetes. Representative traces indicating: (A) Rod responses using 0.01 cd.s/m² flash. (B) Mixed response using 3 cd.s/m² flash. (C) Photopic responses using 3 cd.s/m² flash. (D) Photopic 30 Hz flicker response. (E) Photopic S-cone response using 0.0045cd.s/m² blue flash on an orange background. (TIF)

S2 Fig. Individual presentation of retina function (electroretinograms) of *Psammomys obesus*, control 2, at 28 weeks following the onset of diabetes. Representative traces indicating: (A) Rod responses using 0.01 cd.s/m² flash. (B) Mixed response using 3 cd.s/m² flash. (C) Photopic responses using 3 cd.s/m² flash. (D) Photopic 30 Hz flicker response. (E) Photopic S-cone response using 0.0045cd.s/m² blue flash on an orange background. (TIF)

S3 Fig. Individual presentation of retina function (electroretinograms) of *Psammomys obesus*, control 3, at 28 weeks following the onset of diabetes. Representative traces indicating: (A) Rod responses using 0.01 cd.s/m² flash. (B) Mixed response using 3 cd.s/m² flash. (C) Photopic responses using 3 cd.s/m² flash. (D) Photopic 30 Hz flicker response. (E) Photopic S-cone response using 0.0045cd.s/m² blue flash on an orange background. (TIF)

S4 Fig. Individual presentation of retina function (electroretinograms) of *Psammomys obesus*, control 4, at 28 weeks following the onset of diabetes. Representative traces indicating: (A) Rod responses using 0.01 cd.s/m² flash. (B) Mixed response using 3 cd.s/m² flash. (C) Photopic responses using 3 cd.s/m² flash. (D) Photopic 30 Hz flicker response. (E) Photopic S-cone response using 0.0045cd.s/m² blue flash on an orange background. (TIF)

S5 Fig. Individual presentation of retina function (electroretinograms) of *Psammomys obesus*, control 5, at 28 weeks following the onset of diabetes. Representative traces indicating: (A) Rod responses using 0.01 cd.s/m² flash. (B) Mixed response using 3 cd.s/m² flash. (C) Photopic responses using 3 cd.s/m² flash. (D) Photopic 30 Hz flicker response. (E) Photopic S-cone response using 0.0045cd.s/m² blue flash on an orange background. (TIF)

S6 Fig. Individual presentation of retina function (electroretinograms) of *Psammomys obesus*, control 6, at 28 weeks following the onset of diabetes. Representative traces indicating: (A) Rod responses using 0.01 cd.s/m² flash. (B) Mixed response using 3 cd.s/m² flash. (C) Photopic responses using 3 cd.s/m² flash. (D) Photopic 30 Hz flicker response. (E) Photopic S-cone response using 0.0045cd.s/m² blue flash on an orange background. (TIF)

S7 Fig. Individual presentation of retina function (electroretinograms) of *Psammomys obesus*, diabetic 1, at 28 weeks following the onset of diabetes. Representative traces indicating: (A) Rod responses using 0.01 cd.s/m² flash. (B) Mixed response using 3 cd.s/m² flash. (C) Photopic responses using 3 cd.s/m² flash. (D) Photopic 30 Hz flicker response. (E) Photopic S-cone response using 0.0045cd.s/m² blue flash on an orange background. (TIF)

S8 Fig. Individual presentation of retina function (electroretinograms) of *Psammomys obesus*, diabetic 2, at 28 weeks following the onset of diabetes. Representative traces indicating: (A) Rod responses using 0.01 cd.s/m² flash. (B) Mixed response using 3 cd.s/m² flash. (C) Photopic responses using 3 cd.s/m² flash. (D) Photopic 30 Hz flicker response. (E) Photopic S-cone response using 0.0045cd.s/m² blue flash on an orange background. (TIF)

S9 Fig. Individual presentation of retina function (electroretinograms) of *Psammomys obesus*, diabetic 3, at 28 weeks following the onset of diabetes. Representative traces indicating: (A) Rod responses using 0.01 cd.s/m² flash. (B) Mixed response using 3 cd.s/m² flash. (C) Photopic responses using 3 cd.s/m² flash. (D) Photopic 30 Hz flicker response. (E) Photopic S-cone response using 0.0045cd.s/m² blue flash on an orange background. (TIF)

S10 Fig. Individual presentation of retina function (electroretinograms) of *Psammomys obesus*, diabetic 4, at 28 weeks following the onset of diabetes. Representative traces indicating: (A) Rod responses using 0.01 cd.s/m² flash. (B) Mixed response using 3 cd.s/m² flash. (C)

Photopic responses using 3 cd.s/m² flash. (D) Photopic 30 Hz flicker response. (E) Photopic S-cone response using 0.0045cd.s/m² blue flash on an orange background. (TIF)

S11 Fig. Individual presentation of retina function (electroretinograms) of *Psammomys obesus*, diabetic 5, at 28 weeks following the onset of diabetes. Representative traces indicating: (A) Rod responses using 0.01 cd.s/m² flash. (B) Mixed response using 3 cd.s/m² flash. (C) Photopic responses using 3 cd.s/m² flash. (D) Photopic 30 Hz flicker response. (E) Photopic S-cone response using 0.0045cd.s/m² blue flash on an orange background. (TIF)

S12 Fig. Individual presentation of retina function (electroretinograms) of *Psammomys obesus*, diabetic 6, at 28 weeks following the onset of diabetes. Representative traces indicating: (A) Rod responses using 0.01 cd.s/m² flash. (B) Mixed response using 3 cd.s/m² flash. (C) Photopic responses using 3 cd.s/m² flash. (D) Photopic 30 Hz flicker response. (E) Photopic S-cone response using 0.0045cd.s/m² blue flash on an orange background. (TIF)

Acknowledgments

This work was done within the MOBIDOC program launched under the Support Project to the Research and Innovation System (PASRI) funded by the European Union (EU) and managed by the National Agency for the Promotion of Scientific Research (ANPR) in partnership with UNIMED Laboratories. We wish to thank the Ministry of Tunisian Agriculture (Forest direction) for their authorization to experiment on animals and their help to capture animals.

Author Contributions

Conceptualization: Ahmed Dellaa, Maha Benlarbi, Imane Hammoum, Rafika Ben Chaouacha-Chekir.

Data curation: Ahmed Dellaa, Nouha Gammoudi, Mohamed Dogui.

Formal analysis: Ahmed Dellaa, Imane Hammoum, Riadh Messaoud, Moncef Khairallah, Pierre Lachapelle, Rafika Ben Chaouacha-Chekir.

Funding acquisition: Ahmed Dellaa.

Investigation: Ahmed Dellaa, Imane Hammoum, Nouha Gammoudi, Rafika Ben Chaouacha-Chekir.

Methodology: Ahmed Dellaa, Maha Benlarbi, Imane Hammoum, Riadh Messaoud, Rafika Ben Chaouacha-Chekir.

Project administration: Maha Benlarbi, Rached Azaiz, Ridha Charfeddine, Rafika Ben Chaouacha-Chekir.

Resources: Mohamed Dogui, Ridha Charfeddine, Moncef Khairallah, Rafika Ben Chaouacha-Chekir.

Software: Ahmed Dellaa, Mohamed Dogui.

Supervision: Maha Benlarbi, Riadh Messaoud, Rached Azaiz, Ridha Charfeddine, Rafika Ben Chaouacha-Chekir.

Validation: Pierre Lachapelle, Rafika Ben Chaouacha-Chekir.

Visualization: Ahmed Dellaa, Imane Hammoum, Mohamed Dogui, Rached Azaiz, Ridha Charfeddine, Moncef Khairallah, Pierre Lachapelle, Rafika Ben Chaouacha-Chekir.

Writing – original draft: Ahmed Dellaa, Maha Benlarbi, Pierre Lachapelle, Rafika Ben Chaouacha-Chekir.

Writing – review & editing: Ahmed Dellaa, Pierre Lachapelle, Rafika Ben Chaouacha-Chekir.

References

1. Larsson J, Bauer B, Andreasson S. The 30-Hz flicker cone ERG for monitoring the early course of central retinal vein occlusion. *Acta Ophthalmol Scand*. 2000; 78(2):187–90. PMID: [10794254](#).
2. Brownlee M. Biochemistry and molecular cell biology of diabetic complications. *Nature*. 2001; 414(6865):813–20. <https://doi.org/10.1038/414813a> PMID: [11742414](#).
3. King GL, Shiba T, Oliver J, Inoguchi T, Bursell SE. Cellular and molecular abnormalities in the vascular endothelium of diabetes mellitus. *Annu Rev Med*. 1994; 45:179–88. <https://doi.org/10.1146/annurev.med.45.1.179> PMID: [8198375](#).
4. Lu M, Adamis AP. Vascular endothelial growth factor gene regulation and action in diabetic retinopathy. *Ophthalmol Clin North Am*. 2002; 15(1):69–79. PMID: [12064083](#).
5. Mathews MK, Merges C, McLeod DS, Luttly GA. Vascular endothelial growth factor and vascular permeability changes in human diabetic retinopathy. *Invest Ophthalmol Vis Sci*. 1997; 38(13):2729–41. PMID: [9418725](#).
6. Barber AJ. A new view of diabetic retinopathy: a neurodegenerative disease of the eye. *Prog Neuropsychopharmacol Biol Psychiatry*. 2003; 27(2):283–90. [https://doi.org/10.1016/S0278-5846\(03\)00023-X](https://doi.org/10.1016/S0278-5846(03)00023-X) PMID: [12657367](#).
7. Barber AJ, Lieth E, Khin SA, Antonetti DA, Buchanan AG, Gardner TW. Neural apoptosis in the retina during experimental and human diabetes. Early onset and effect of insulin. *J Clin Invest*. 1998; 102(4):783–91. <https://doi.org/10.1172/JCI2425> PMID: [9710447](#).
8. Lieth E, Gardner TW, Barber AJ, Antonetti DA, Penn State Retina Research G. Retinal neurodegeneration: early pathology in diabetes. *Clin Experiment Ophthalmol*. 2000; 28(1):3–8. PMID: [11345341](#).
9. Lopes de Faria JM, Russ H, Costa VP. Retinal nerve fibre layer loss in patients with type 1 diabetes mellitus without retinopathy. *Br J Ophthalmol*. 2002; 86(7):725–8. PMID: [12084737](#).
10. Martin PM, Roon P, Van Ellis TK, Ganapathy V, Smith SB. Death of retinal neurons in streptozotocin-induced diabetic mice. *Invest Ophthalmol Vis Sci*. 2004; 45(9):3330–6. <https://doi.org/10.1167/iovs.04-0247> PMID: [15326158](#).
11. Feitosa-Santana C, Paramei GV, Nishi M, Gualtieri M, Costa MF, Ventura DF. Color vision impairment in type 2 diabetes assessed by the D-15d test and the Cambridge Colour Test. *Ophthalmic Physiol Opt*. 2010; 30(5):717–23. <https://doi.org/10.1111/j.1475-1313.2010.00776.x> PMID: [20883359](#).
12. Gualtieri M, Feitosa-Santana C, Lago M, Nishi M, Ventura DF. Early visual changes in diabetic patients with no retinopathy measured by color discrimination and electroretinography. *Psychology & Neuroscience*. 2013; 6:227–34.
13. Boynton GE, Stem MS, Kwark L, Jackson GR, Farsiu S, Gardner TW. Multimodal characterization of proliferative diabetic retinopathy reveals alterations in outer retinal function and structure. *Ophthalmology*. 2015; 122(5):957–67. <https://doi.org/10.1016/j.ophtha.2014.12.001> PMID: [25601533](#).
14. Kizawa J, Machida S, Kobayashi T, Gotoh Y, Kurosaka D. Changes of oscillatory potentials and photopic negative response in patients with early diabetic retinopathy. *Jpn J Ophthalmol*. 2006; 50(4):367–73. <https://doi.org/10.1007/s10384-006-0326-0> PMID: [16897223](#).
15. Okuno T, Oku H, Sugiyama T, Ikeda T. Electroretinographic study of spontaneously diabetic Torii rats. *Doc Ophthalmol*. 2008; 117(3):191–6. <https://doi.org/10.1007/s10633-008-9122-0> PMID: [18343964](#).
16. Klemp K, Sander B, Brockhoff PB, Vaag A, Lund-Andersen H, Larsen M. The multifocal ERG in diabetic patients without retinopathy during euglycemic clamping. *Investigative ophthalmology & visual science*. 2005; 46(7):2620–6.
17. Rungger-Brandle E, Dosso AA, Leuenberger PM. Glial reactivity, an early feature of diabetic retinopathy. *Invest Ophthalmol Vis Sci*. 2000; 41(7):1971–80. PMID: [10845624](#).
18. Tzekov R, Arden GB. The electroretinogram in diabetic retinopathy. *Surv Ophthalmol*. 1999; 44(1):53–60. PMID: [10466588](#).
19. Bresnick GH, Palta M. Oscillatory potential amplitudes. Relation to severity of diabetic retinopathy. *Arch Ophthalmol*. 1987; 105(7):929–33. PMID: [3606452](#).

20. Simonsen SE. The value of the oscillatory potential in selecting juvenile diabetics at risk of developing proliferative retinopathy. *Acta Ophthalmol (Copenh)*. 1980; 58(6):865–78. PMID: [7331773](#).
21. Hancock HA, Kraft TW. Oscillatory potential analysis and ERGs of normal and diabetic rats. *Invest Ophthalmol Vis Sci*. 2004; 45(3):1002–8. PMID: [14985323](#).
22. Layton CJ, Chidlow G, Casson RJ, Wood JP, Graham M, Osborne NN. Monocarboxylate transporter expression remains unchanged during the development of diabetic retinal neuropathy in the rat. *Invest Ophthalmol Vis Sci*. 2005; 46(8):2878–85. <https://doi.org/10.1167/iovs.04-1458> PMID: [16043862](#).
23. Li Q, Zemel E, Miller B, Perlman I. Early retinal damage in experimental diabetes: electroretinographical and morphological observations. *Exp Eye Res*. 2002; 74(5):615–25. <https://doi.org/10.1006/exer.2002.1170> PMID: [12076083](#).
24. Phipps JA, Fletcher EL, Vingrys AJ. Paired-flash identification of rod and cone dysfunction in the diabetic rat. *Invest Ophthalmol Vis Sci*. 2004; 45(12):4592–600. <https://doi.org/10.1167/iovs.04-0842> PMID: [15557472](#).
25. MacGregor LC, Matschinsky FM. Experimental diabetes mellitus impairs the function of the retinal pigmented epithelium. *Metabolism*. 1986; 35(4 Suppl 1):28–34. PMID: [3007925](#).
26. Viswanathan S, Frishman L, editors. Evidence that negative potentials in the photopic electroretinograms of cats and primates depend upon spiking activity of retinal ganglion cell axons. *Soc Neurosci Abstr*; 1997.
27. Saidi T, Mbarek S, Omri S, Behar-Cohen F, Chaouacha-Chekir RB, Hicks D. The sand rat, *Psammomys obesus*, develops type 2 diabetic retinopathy similar to humans. *Invest Ophthalmol Vis Sci*. 2011; 52(12):8993–9004. <https://doi.org/10.1167/iovs.11-8423> PMID: [21989730](#).
28. Saidi T, Chaouacha-Chekir R, Hicks D. Advantages of *Psammomys obesus* as an Animal Model to Study Diabetic Retinopathy. *J Diabetes Metab*. 2012; 3(207):2.
29. Dellaa A, Polosa A, Mbarek S, Hammoum I, Messaoud R, Amara S, et al. Characterizing the Retinal Function of *Psammomys obesus*: A Diurnal Rodent Model to Study Human Retinal Function. *Curr Eye Res*. 2016:1–9. <https://doi.org/10.3109/02713683.2016.1141963> PMID: [27216715](#).
30. McCulloch DL, Marmor MF, Brigell MG, Hamilton R, Holder GE, Tzekov R, et al. Erratum to: ISCEV Standard for full-field clinical electroretinography (2015 update). *Doc Ophthalmol*. 2015; 131(1):81–3. <https://doi.org/10.1007/s10633-015-9504-z> PMID: [26059396](#).
31. Saidi T, Mbarek S, Chaouacha-Chekir RB, Hicks D. Diurnal rodents as animal models of human central vision: characterisation of the retina of the sand rat *Psammomys obesus*. *Graefes Arch Clin Exp Ophthalmol*. 2011; 249(7):1029–37. <https://doi.org/10.1007/s00417-011-1641-9> PMID: [21399940](#).
32. Raz I, Wexler I, Weiss O, Flyvbjerg A, Segev Y, Rauchwerger A, et al. Role of insulin and the IGF system in renal hypertrophy in diabetic *Psammomys obesus* (sand rat). *Nephrol Dial Transplant*. 2003; 18(7):1293–8. PMID: [12808164](#).
33. Sahraoui A, Dewachter C, de Medina G, Naeije R, Aouichat Bouguerra S, Dewachter L. Myocardial Structural and Biological Anomalies Induced by High Fat Diet in *Psammomys obesus* Gerbils. *PLoS One*. 2016; 11(2):e0148117. <https://doi.org/10.1371/journal.pone.0148117> PMID: [26840416](#).
34. Hammoum I, Mbarek S, Dellaa A, Dubus E, Baccouche B, Azaiz R, et al. Study of retinal alterations in a high fat diet-induced type ii diabetes rodent: Meriones shawi. *Acta Histochemica*. <http://dx.doi.org/10.1016/j.acthis.2016.05.005>.
35. Baccouche B, Mbarek S, Dellaa A, Hammoum I, Messina CM, Santulli A, et al. Protective Effect of Astaxanthin on Primary Retinal Cells of the Gerbil *Psammomys Obesus* Cultured in Diabetic Milieu. *Journal of Food Biochemistry*. 2016:n/a–n/a. <https://doi.org/10.1111/jfbc.12274>
36. Chung NH, Kim SH, Kwak MS. The electroretinogram sensitivity in patients with diabetes. *Korean J Ophthalmol*. 1993; 7(2):43–7. PMID: [8189633](#).
37. Bloodworth JM Jr. Diabetic retinopathy. *Diabetes*. 1962; 11:1–22. PMID: [13870120](#).
38. Juen S, Kieselbach GF. Electrophysiological changes in juvenile diabetics without retinopathy. *Arch Ophthalmol*. 1990; 108(3):372–5. PMID: [2310337](#).
39. Arden GB, Sivaprasad S. The pathogenesis of early retinal changes of diabetic retinopathy. *Doc Ophthalmol*. 2012; 124(1):15–26. <https://doi.org/10.1007/s10633-011-9305-y> PMID: [22302291](#).
40. Heckenlively JR. New concept: treating nonproliferative diabetic retinopathy with light adaptation of rods during sleep. *Eye (Lond)*. 2011; 25(12):1533–4. <https://doi.org/10.1038/eye.2011.263> PMID: [22056867](#).
41. Holopigian K, Seiple W, Lorenzo M, Carr R. A comparison of photopic and scotopic electroretinographic changes in early diabetic retinopathy. *Invest Ophthalmol Vis Sci*. 1992; 33(10):2773–80. PMID: [1526726](#).

42. Jaissle GB, May CA, Reinhard J, Kohler K, Fauser S, Lutjen-Drecoll E, et al. Evaluation of the rhodopsin knockout mouse as a model of pure cone function. *Invest Ophthalmol Vis Sci*. 2001; 42(2):506–13. PMID: [11157890](#).
43. Aizu Y, Katayama H, Takahama S, Hu J, Nakagawa H, Oyanagi K. Topical instillation of ciliary neurotrophic factor inhibits retinal degeneration in streptozotocin-induced diabetic rats. *Neuroreport*. 2003; 14(16):2067–71. <https://doi.org/10.1097/01.wnr.0000097044.56589.78> PMID: [14600499](#).
44. Kern TS, Miller CM, Tang J, Du Y, Ball SL, Berti-Matera L. Comparison of three strains of diabetic rats with respect to the rate at which retinopathy and tactile allodynia develop. *Mol Vis*. 2010; 16:1629–39. PMID: [20806092](#).
45. Pautler EL, Ennis SR. The effect of induced diabetes on the electroretinogram components of the pigmented rat. *Invest Ophthalmol Vis Sci*. 1980; 19(6):702–5. PMID: [7380629](#).
46. Sakai H, Tani Y, Shirasawa E, Shirao Y, Kawasaki K. Development of electroretinographic alterations in streptozotocin-induced diabetes in rats. *Ophthalmic Res*. 1995; 27(1):57–63. PMID: [7596561](#).
47. Wachtmeister L. Oscillatory potentials in the retina: what do they reveal. *Prog Retin Eye Res*. 1998; 17(4):485–521. PMID: [9777648](#).
48. Wachtmeister L, Dowling JE. The oscillatory potentials of the mudpuppy retina. *Invest Ophthalmol Vis Sci*. 1978; 17(12):1176–88. PMID: [721390](#).
49. Dorfman AL, Dembinska O, Chemtob S, Lachapelle P. Structural and functional consequences of trolox C treatment in the rat model of postnatal hyperoxia. *Invest Ophthalmol Vis Sci*. 2006; 47(3):1101–8. <https://doi.org/10.1167/iovs.05-0727> PMID: [16505047](#).
50. Luu CD, Szental JA, Lee S-Y, Lavanya R, Wong TY. Correlation between retinal oscillatory potentials and retinal vascular caliber in type 2 diabetes. *Investigative ophthalmology & visual science*. 2010; 51(1):482–6.
51. Shirao Y, Kawasaki K. Electrical responses from diabetic retina. *Prog Retin Eye Res*. 1998; 17(1):59–76. PMID: [9537795](#).
52. Bresnick GH, Korth K, Groo A, Palta M. Electroretinographic oscillatory potentials predict progression of diabetic retinopathy. Preliminary report. *Arch Ophthalmol*. 1984; 102(9):1307–11. PMID: [6383303](#).
53. Coupland SG. A comparison of oscillatory potential and pattern electroretinogram measures in diabetic retinopathy. *Doc Ophthalmol*. 1987; 66(3):207–18. PMID: [3428075](#).
54. Yonemura D, Aoki T, Tsuzuki K. Electroretinogram in diabetic retinopathy. *Arch Ophthalmol*. 1962; 68:19–24. PMID: [14009176](#).
55. Bresnick GH, Palta M. Temporal aspects of the electroretinogram in diabetic retinopathy. *Arch Ophthalmol*. 1987; 105(5):660–4. PMID: [3619742](#).
56. Bresnick GH, Palta M. Predicting progression to severe proliferative diabetic retinopathy. *Arch Ophthalmol*. 1987; 105(6):810–4. PMID: [3579713](#).
57. Vadala M, Anastasi M, Lodato G, Cillino S. Electroretinographic oscillatory potentials in insulin-dependent diabetes patients: A long-term follow-up. *Acta Ophthalmol Scand*. 2002; 80(3):305–9. PMID: [12059871](#).
58. Hombrebueno JR, Chen M, Penalva RG, Xu H. Loss of synaptic connectivity, particularly in second order neurons is a key feature of diabetic retinal neuropathy in the *Ins2Akita* mouse. *PLoS One*. 2014; 9(5):e97970. <https://doi.org/10.1371/journal.pone.0097970> PMID: [24848689](#).
59. Shinoda K, Rejdak R, Schuettauf F, Blatsios G, Volker M, Tanimoto N, et al. Early electroretinographic features of streptozotocin-induced diabetic retinopathy. *Clin Experiment Ophthalmol*. 2007; 35(9):847–54. <https://doi.org/10.1111/j.1442-9071.2007.01607.x> PMID: [18173414](#).
60. Ishikawa A, Ishiguro S, Tamai M. Changes in GABA metabolism in streptozotocin-induced diabetic rat retinas. *Curr Eye Res*. 1996; 15(1):63–71. PMID: [8631205](#).
61. Rufiange M, Dassa J, Dembinska O, Koenekoop RK, Little JM, Polomeno RC, et al. The photopic ERG luminance-response function (photopic hill): method of analysis and clinical application. *Vision Res*. 2003; 43(12):1405–12. Epub 2003/05/14. PMID: [12742110](#).
62. Rosolen SG, Rigaudiere F, LeGargasson JF, Chalier C, Rufiange M, Racine J, et al. Comparing the photopic ERG i-wave in different species. *Vet Ophthalmol*. 2004; 7(3):189–92. Epub 2004/04/20. <https://doi.org/10.1111/j.1463-5224.2004.04022.x> PMID: [15091327](#).
63. Yang S, Luo X, Xiong G, So KF, Yang H, Xu Y. The electroretinogram of Mongolian gerbil (*Meriones unguiculatus*): comparison to mouse. *Neurosci Lett*. 2015; 589:7–12. Epub 2015/01/13. <https://doi.org/10.1016/j.neulet.2015.01.018> PMID: [25578951](#).
64. Govardovskii VI, Rohlich P, Szel A, Khokhlova TV. Cones in the retina of the Mongolian gerbil, *Meriones unguiculatus*: an immunocytochemical and electrophysiological study. *Vision Res*. 1992; 32(1):19–27. Epub 1992/01/01. PMID: [1502806](#).

65. Szel A, Rohlich P. Two cone types of rat retina detected by anti-visual pigment antibodies. *Exp Eye Res.* 1992; 55(1):47–52. Epub 1992/07/01. PMID: [1397129](#).
66. Carter-Dawson LD, LaVail MM. Rods and cones in the mouse retina. I. Structural analysis using light and electron microscopy. *J Comp Neurol.* 1979; 188(2):245–62. Epub 1979/11/15. <https://doi.org/10.1002/cne.901880204> PMID: [500858](#).
67. Rousseau S, McKerral M, Lachapelle P. The i-wave: bridging flash and pattern electroretinography. *Electroencephalogr Clin Neurophysiol Suppl.* 1996; 46:165–71. Epub 1996/01/01. PMID: [9059790](#).
68. Viswanathan S, Frishman LJ, Robson JG, Harwerth RS, Smith EL 3rd. The photopic negative response of the macaque electroretinogram: reduction by experimental glaucoma. *Invest Ophthalmol Vis Sci.* 1999; 40(6):1124–36. PMID: [10235545](#).
69. Viswanathan S, Frishman LJ, Robson JG, Walters JW. The photopic negative response of the flash electroretinogram in primary open angle glaucoma. *Invest Ophthalmol Vis Sci.* 2001; 42(2):514–22. PMID: [11157891](#).
70. Chen H, Zhang M, Huang S, Wu D. The photopic negative response of flash ERG in nonproliferative diabetic retinopathy. *Doc Ophthalmol.* 2008; 117(2):129–35. <https://doi.org/10.1007/s10633-008-9114-0> PMID: [18214565](#).
71. Kim HD, Park JY, Ohn YH. Clinical applications of photopic negative response (PhNR) for the treatment of glaucoma and diabetic retinopathy. *Korean J Ophthalmol.* 2010; 24(2):89–95. <https://doi.org/10.3341/kjo.2010.24.2.89> PMID: [20379458](#).
72. Ghirlanda G, Di Leo MA, Caputo S, Falsini B, Porciatti V, Marietti G, et al. Detection of inner retina dysfunction by steady-state focal electroretinogram pattern and flicker in early IDDM. *Diabetes.* 1991; 40(9):1122–7. PMID: [1936619](#).
73. Tahara K, Matsuura T, Otori T. Diagnostic evaluation of diabetic retinopathy by 30-Hz flicker electroretinography. *Jpn J Ophthalmol.* 1993; 37(2):204–10. PMID: [8230847](#).
74. Satoh S, Iijima H, Imai M, Abe K, Shibuya T. Photopic electroretinogram implicit time in diabetic retinopathy. *Jpn J Ophthalmol.* 1994; 38(2):178–84. PMID: [7967210](#).
75. Mortlock KE, Chiti Z, Drasdo N, Owens DR, North RV. Silent substitution S-cone electroretinogram in subjects with diabetes mellitus. *Ophthalmic Physiol Opt.* 2005; 25(5):392–9. <https://doi.org/10.1111/j.1475-1313.2005.00299.x> PMID: [16101944](#).
76. Yamamoto S, Kamiyama M, Nitta K, Yamada T, Hayasaka S. Selective reduction of the S cone electroretinogram in diabetes. *Br J Ophthalmol.* 1996; 80(11):973–5. PMID: [8976724](#).